Proceedings of ASME Turbo Expo 2011
GT2011
June 6-10, 2011, Vancouver, British Columbia, Canada

GT2011-46015

NUMERICAL INVESTIGATION OF DIFFERENT CASING TREATMENTS ON PERFORMANCE OF A HIGH SPEED CENTRIFUGAL COMPRESSOR STAGE

Yan Ma, Guang Xi
School of Energy and Power Engineering, Xi'an Jiaotong University, Xi'an 710049, P. R. China
E-mail: xiguang@mail.xjtu.edu.cn
Guangkuan Wu
Institute of Water Resources and Hydro-electric Engineering, Xi'an University of Technology, Xi'an 710048, P.R. China

ABSTRACT

In this paper, two different casing treatment devices—one adopting inlet recirculation at the shroud side of the impeller inlet and the other adopting circumferential casing grooves at the shroud side of the vaneless space, are designed for a high speed centrifugal compressor stage. The effects of different casing treatments to the flow range and performance of the centrifugal compressor stage are studied numerically.

The results indicate that traditional inlet recirculation at impeller inlet does not extend the stall margin of the stage and the performance deteriorates due to the adding of the extra device. The study also shows that, when the location of the bleed slot moves downstream, the performance of the stage deteriorates due to the longer flow path.

Moreover, the 2mm depth circumferential casing grooves extend the stall margin by about 12.05%. By contrast, the 6mm depth and 10mm depth grooves extend the stall margin by 3% and 2.4% respectively.

NOMENCALTURE

b	Blade height (mm)
D	Diameter (mm)
N	Rotational speed (rpm)
Z	Blade/Vane number
CCG	Circumferential casing grooves
IR	Inlet recirculation

Greek letters

ϕ	Mass flow rate (g/s)

Subscript

0	Impeller inlet tip
2	Impeller outlet
3	Diffuser inlet
4	Diffuser outlet
des	Design point

INTRODUCTION

Centrifugal compressors are used widely in the fields of aviation industry, chemical and petroleum industry, metallurgical industry, and small gas turbines. When operating below the design mass flow rate, centrifugal compressor is likely to have severe vibrations due to stall and surge. This would cause instability problem of the compressor and would reduce its performance. Thus, in the design of a centrifugal compressor, enhancing stall margin should be an important consideration. [1-3].

As a passive flow control method, casing treatment has been used in practice for years to enhance the operating range of the compressor. Many researchers have investigated various types of casing treatment to achieve a wide flow range in axial and centrifugal compressors. The effects of casing treatment have been clarified in detail based on numerical simulations and confirmed experiments [4].

The concept of casing treatment was firstly proposed by Koch and Smith, who investigated the impact of upstream blowing and downstream bleeding on the stable operating range of a transonic compressor [5]. Since then, various forms of casing treatments have been designed and their mechanism in expanding the compressor flow range has been investigated by many researchers.

The NASA Glenn Research Center did lots of work related to the inception of rotating stall and casing treatment devices to control stall and extend the stall lines for axial compressors [6-12]. Their recent work reported a passive advanced casing treatment developed for a high-bypass ratio turbofan engine and was tested on a scale model in the 9×15 NASA Glenn Wind Tunnel. The results indicated that all the tested casing treatment configurations increased the stall margin of the engine, while a few of the designs also showed a potential noise benefit for certain engine speeds [12].

For centrifugal compressors, Gary Skoch at NASA GRC did a series of experiments to investigate techniques for expending the stable flow range of a high-speed centrifugal compressor [13, 14]. Spakovszky [15] designed an air injection scheme between the impeller and vaned diffuser for the NASA Glenn CC3 high-speed centrifugal compressor. The results showed an increase of 25% in surge-margin with an injection mass flow of 0.5% of the compressor mass flow. Hu Liangjun et al. [16] designed inducer bleeding, inlet recirculation and circumferential groove casing treatments to enhance the stall margin of a centrifugal compressor. The differences of the performance between solid casing stage and stages with casing treatment devices were compared by using CFD software. The results indicated that all the applied techniques could decrease the flow blockage near the inducer tip and delay the occurrence of stall, but inducer bleeding and inlet recirculation were more effective. The circumferential groove casing treatment device in their research was performed at the inlet part of the impeller. Barton et al. [17] did numerical optimization of a modern centrifugal compressor with an inducer vaned shroud for increased operability margin. The results indicated that the vane shroud did extend compressor surge margin at the part-speed operating condition, while maintaining acceptable high-speed performance. Junfei Yin et al. [18] developed an optimization procedure for ported-shroud compressor based on Design of Experiment (DOE) procedure. The results indicated that the configuration improved map width by 9%, an increased pressure ratio by 0.2 and a higher peak efficiency by about 1%. Tong Wang et al. [19] designed a new type of casing treatment with self-adaptivity to expand the stall margin of centrifugal compressor with unshrouded impeller. Their test results of two types of casing treatments indicated that the method could extend the stall margin by about 20% and slightly increase or maintain the efficiency over the whole operation range. Besides, the mechanism of this method to expand the stall margin was discussed based on experimental and analytical evidence. Other similar research about casing treatment and its effects on centrifugal compressor performance can be found in reference [20-24].

In the present paper, the effects of different casing treatments to the flow range and performance of a high speed centrifugal compressor stage are studied numerically. Firstly, traditional casing treatment device as inlet recirculation at impeller inlet is performed to this centrifugal compressor stage and its effect is discussed. Then, a new type vaneless space casing treatment device is designed and studied. Also, flow analysis in the stage provides guidelines for further redesign of the casing treatment device.

NUMERICAL APPROACH

Numerical Method

3-D flow calculations are performed in the present study by using the software package NUMECA FINE/Turbo^{TM} to predict the performance of the stage and to investigate the flow characteristics [25]. The Spalart-Allmaras model is selected as the turbulence model. The calculations are carried out with second-order central scheme. The numerical procedure adopts a four-stage Runge-Kutta scheme coupled with local time stepping and implicit residual smoothing for convergence acceleration.

The computational domain consists of one impeller passage with a main blade and a splitter blade and one diffuser passage. For the interface between the rotating impeller and the stationary vaned diffuser, the full non-matching mixing plane approach is used. The computational grid was generated with the auto-grid generation software IGG/AutoGrid v8 of NUMECA [26]. In consideration of the computation's fidelity and cost, a mesh independence study was firstly performed. The results suggested that a total of 917,842 nodes for the impeller and 236,433 for the diffuser were sufficient to obtain grid independent values for the figures of merit and can provide enough details for flow analysis. The grid is refined in the near-wall regions and at the leading and trailing edge of the impeller (Fig. 1). For the casing treatment device, the channel grid is generated by using the ZR Effect of AutoGrid. The connection between the casing treatment device and the main flow channel is set to full non-matching boundary (FNMB) (Fig. 2). The near-wall Y^+ is adjusted to less than 3 in the process of grid generating for all the computational cases.

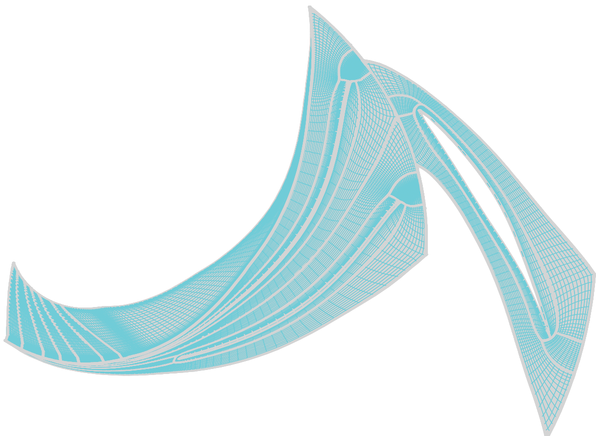

Fig. 1 Computational grid of the baseline stage

At the inlet, uniform total pressure and temperature with axial flow direction are set as boundary condition. The ideal air is considered as working fluid and mass flow is imposed at the computational domain outlet. The hub wall of the impeller moves with the blade, while the whole shroud keeps stationary. Non-slip wall conditions are applied over all solid walls. Periodic conditions are applied for pitchwise boundaries other than the blade surfaces. Steady analyses are performed with the above method. It should be pointed out that usually steady simulation is not suitable for predicting the initiation point of stall precisely as compressor stall is a strongly unsteady process. But as a less CPU time requirement, steady simulation is often used to predict the compressor performance map. The mass flow point where steady simulation begins to diverge is generally considered to be the stall point of the compressor.

Computational Model and Design of the Casing Treatment Devices

The high speed centrifugal compressor stage studied in the present paper has a small mass flow rate and a low pressure ratio with a long and narrow flow passage. Table 1 shows the main specification of the impeller and the diffuser.

Table 1 Specification of the centrifugal compressor stage

Impeller	Inlet tip diameter (D_0)	57mm
	Outlet diameter (D_2)	130mm
	Blade number (Z)	7
	Outlet blade height (b_2)	2.95mm
	Tip clearance size	0.3mm
	Design mass flow rate (ϕ_{des})	67g/s
	Rotational speed (N)	35000rpm
Diffuser	Inlet diameter (D_3)	149.5mm
	Outlet diameter (D_4)	195mm
	Vane number (Z)	17

The flow analysis of the smooth casing stage shows that at the impeller inlet a large vortex appears at the shroud side of the flow passage near stall point. In order to improve both the stall margin and the efficiency of the stage, it is important to control the vortex. Besides, as the flow diffuses in the flow passage and interacts with the tip gap flow, the vortex will cause the flow to separate at the shroud side in the vaneless space and set up a recirculation zone. As the flow passage in the vaneless space is narrow, the appearance of this recirculation zone may also affect the stall margin of the stage. Thus, two different casing treatment devices—one adopted inlet recirculation (IR) at the shroud side of the impeller inlet and the other one adopted circumferential casing grooves (CCG) at the shroud side of the vaneless space, have been designed for this centrifugal compressor stage (Fig. 2 (a), (b)).

The inlet recirculation device consists of a bleed slot, an upstream slot and an annular cavity connecting both slots. The width of the bleed slot is 1.5mm and locates at a distance of 2.5mm downstream of the splitter blade leading edge for IR_1. For IR_2, it locates at a distance of 5.5mm downstream of the splitter blade leading edge. Through the annular cavity, of which the width is 3mm, the bleeding flow is injected into the core flow at a distance of 6.5mm upstream of the main blade leading edge through the upstream slot. The width of the upstream slot is 2.5mm.

For the circumferential casing grooves, the first groove locates at a distance of 2mm downstream of the blade trailing edge; the width of the groove is 2.5mm, with a gap of 1mm between the two grooves. In the present study, three different depths of the grooves are studied, i.e. —2mm, 6mm and 10mm.

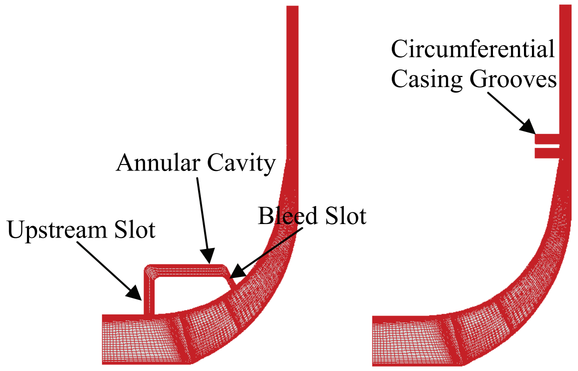

(a) IR_1 **(b) CCG_6mm**

Fig. 2 Sketch map of the casing treatment devices

RESULTS AND DISSCUSSION

Effect of Inlet Recirculation

Inlet recirculation (IR), as its successful applications in many engineering fields, is proved to be an effective way for centrifugal compressor stall margin extension. In the inlet recirculation device, the low-energy flow near the shroud of the impeller is forced to move toward the upstream of the main flow due to the pressure gradient between the bleed and upstream slots. Thus, the incidence angle of the impeller is reduced and the stall margin is enhanced. In the following part, the effect of IR to the performance and stall margin of the centrifugal compressor stage and the influence of the location of the bleed slot are discussed.

Overall Performance

Figure 3 shows the calculated performance characteristics of the smooth casing stage and stages with inlet recirculation device. Table 2 gives all the simulated test cases with the stall mass flow rate and efficiency at design point.

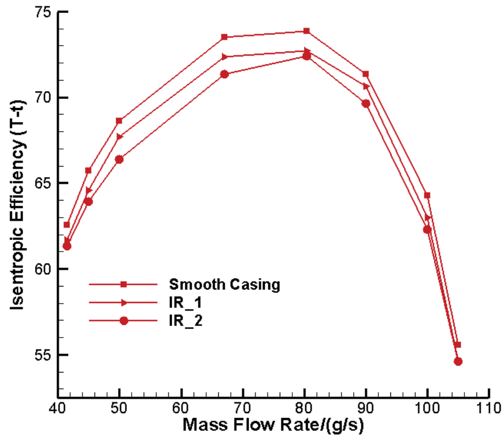

(a) Isentropic Efficiency

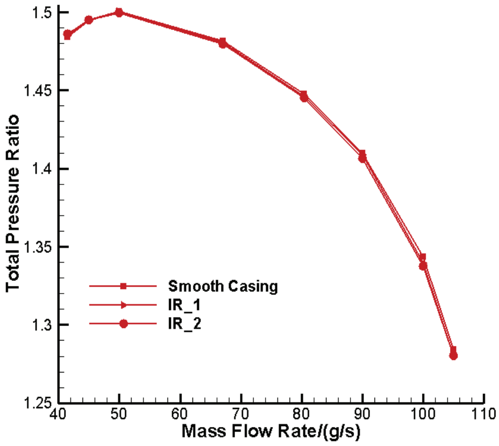

(b) Total Pressure Ratio

Fig. 3 Calculated stage performance characteristics to evaluate the effect of IR

Table 2 Comparison between smooth casing stage and stages with inlet recirculation

	Stall mass flow	Efficiency at design point
Smooth caing	41.5 g/s	73.50%
IR_1	41.5 g/s	72.35%
IR_2	41.5 g/s	71.36%

It can be seen from Figure 3 and Table 2 that the adoption of inlet recirculation does not extend the stall margin of the stage. As the adding of the additional device, the efficiency drops along the whole operating range. The efficiency of the stage with IR_2 drops more due to an even longer flow path in the casing treatment device. The efficiency drops by about 1.15% for IR_1 and by about 2.14% for IR_2 at design mass flow rate. But the adoption of inlet recirculation has minor effect on the total pressure ratio of the stage.

Flow fields at $\phi = 41.5$g/s , the stall point of the smooth casing stage

Figure 4 shows the circumferentially mass averaged streamlines and static pressure distribution at the meridional plane of the smooth casing stage and stages with inlet recirculation device. It can be seen from the figure that the adoption of inlet recirculation plays the role of guiding the low-energy flow near the shroud of the impeller to move toward the upstream of the main flow. But the area of the large vortex at the impeller inlet does not reduce no matter with IR_1 or IR_2. The reason may be the low pressure gradient along the impeller shroud. In other words, the low energy fluid cannot obtain enough energy to recirculate through the casing treatment device. Thus, the effect of inlet recirculation is restricted.

Figure 5 gives more flow details in the inlet recirculation device. The figure shows that two vortexes appear in the inlet recirculation devices for both IR_1 and IR_2. One locates at the upper turning corner of the bleed slot. The other locates at the bottom part of the annular cavity. The appearance of the vortexes will deteriorate the flow status in the inlet recirculation device and will arouse more losses, thus corresponding to a higher entropy value. Therefore, the configurations of the inlet recirculation devices need to be redesigned for a better flow condition. For IR_2, the entropy value throughout the whole casing treatment device is higher than IR_1, thus its efficiency is lower.

Figure 6 shows the entropy contours at 90% span in the impeller passage. For the smooth casing impeller, a large high entropy zone appears at the rear part of the impeller passage, especially near the pressure side of the impeller blade. This high entropy zone is induced by the mixing of the tip leakage flow with the main flow.

As for the adoption of the inlet recirculation device, the entropy value at impeller inlet rises compared with the smooth casing impeller due to flow mixing at impeller inlet. The existence of the bleed slot weakens the separated flow at the middle part of the main blade and near the leading edge part of the splitter blade (indicated by the red circles in the figure). Hence the entropy value reduces. Near the rear part of the impeller blade pressure side, the range of the high entropy region expands.

From the figure of the entropy distribution along with streamlines at 90% span in the diffuser passage in Figure 7, we can see that the adoption of inlet recirculation does not change the flow status in the diffuser passage. But as the adding of the extra device, the entropy value rises throughout the diffuser passage and this will induce more losses. As far as the average entropy value in the stage, the stages with IR are higher than the smooth casing stage, thus their efficiency are lower.

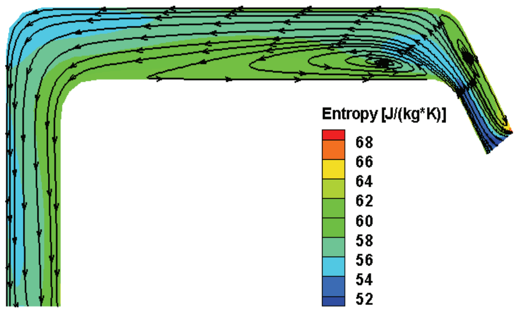

(a). IR_1

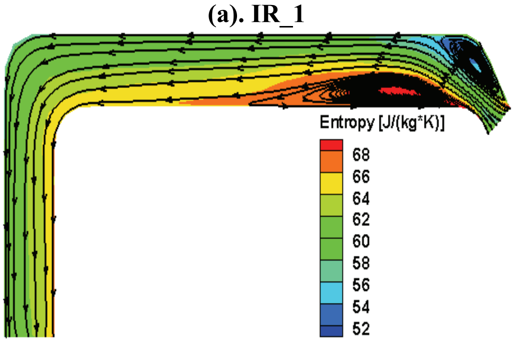

(b). IR_2

Fig. 5 Streamlines and entropy distribution in IR device (Mass averaged)

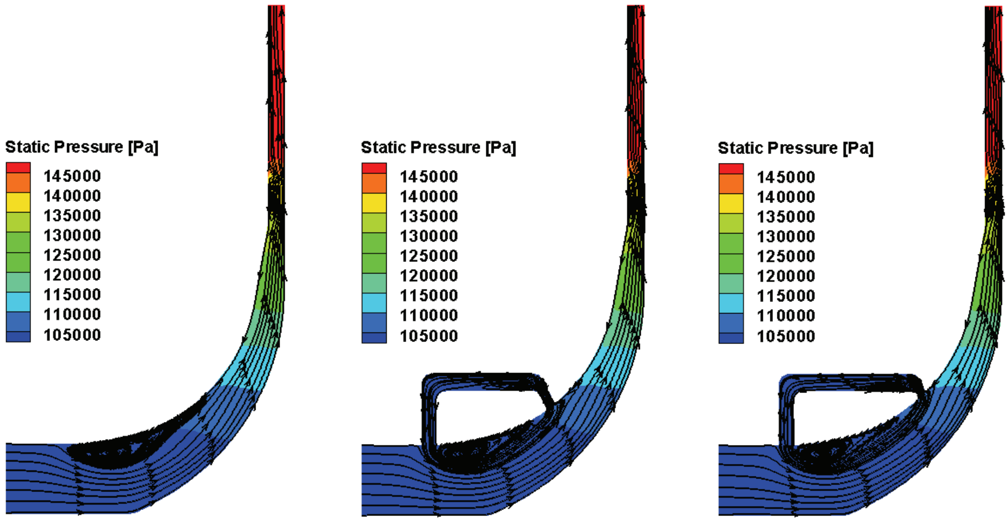

(a). Smooth Casing (b). IR_1 (c). IR_2

Fig. 4 Streamlines and static pressure distribution at the meridional plane (Mass average)

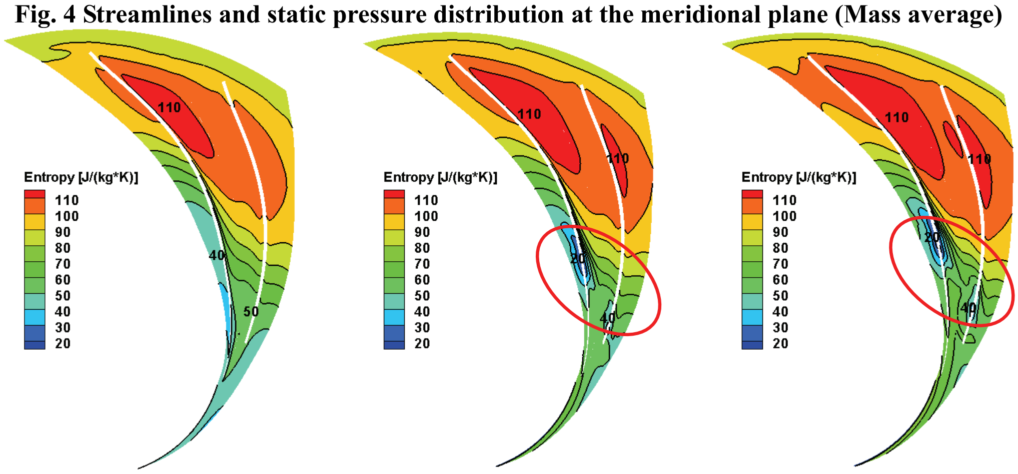

(a). Smooth Casing (b). IR_1 (c). IR_2

Fig. 6 Entropy distribution in the impeller passage at 90% span

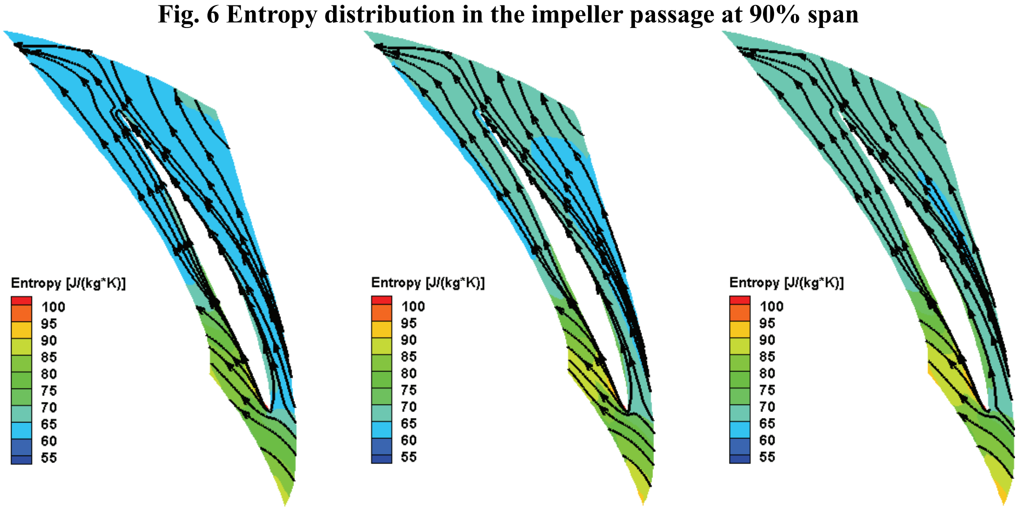

(a). Smooth Casing (b). IR_1 (c). IR_2

Fig. 7 Streamlines and entropy distribution in the diffuser passage at 90% span

Effect of Circumferential Casing Grooves

Circumferential casing grooves (CCG), as one of the passive methods to control compressor stall, is known to increase the stall margin by delaying stall [2]. The main feature of the CCG device proposed in the present paper is that it locates at the stationary part of the stage, thus is easy to implement. The following part focuses on the effects of groove depth to the stall margin and performance of the centrifugal compressor stage.

Overall Performance

Figure 8 shows the calculated performance characteristics of the smooth casing stage and stages with different depth grooves. Table 3 lists all the simulated test cases with the stall mass flow rate, efficiency at design point and stall margin improvement. According to Takata [27], the percent improvement of the stall margin is defined as:

$$\Delta\phi = 1 - \phi_{rs2} / \phi_{rs1} , \tag{1}$$

here ϕ_{rs1} and ϕ_{rs2} refers to the stall mass flow of the smoothing casing stage and stage with casing treatment.

As shown in Figure 8 and Table 3, the percent improvement of the stall margin is about 12.05%, 2.41% and 3.01% for the stages with 2mm, 6mm and 10mm depth grooves respectively. Thus, the 2mm depth grooves have the best effect in terms of expanding the stall margin of the stage.

In consideration of the efficiency and total pressure ratio, the stage with 6mm depth grooves shows the best performance. For the stage with 6mm depth grooves, the efficiency drops slightly compared with the smooth casing stage for the calculated mass flow except for the points near stall point. The efficiency drops by about 0.63% at design mass flow. For the stage with 2mm and 10mm depth grooves, the values are 5.34% and 6.10% respectively. The total pressure ratio of the stage with 6mm depth grooves decreases slightly as compared with the smooth casing stage. As for the stages with 2mm and 10mm depth grooves, remarkable decreases of total pressure ratio are observed. As the total pressure ratio differences between the two configurations are so small, a partial enlarged view near the stall point is given near the upper right corner of Figure 8(b).

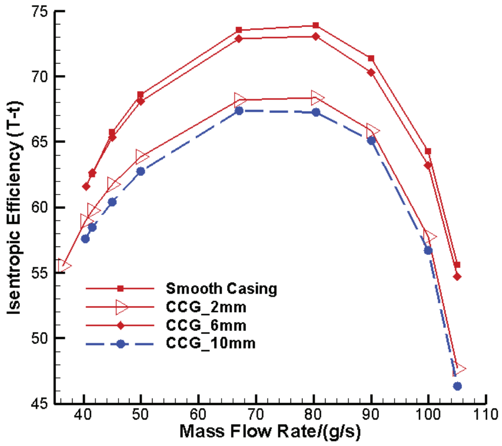

(a) Isentropic Efficiency

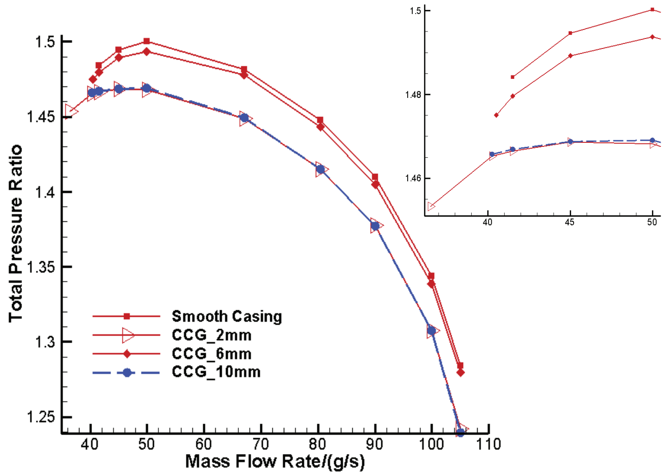

(b) Total Pressure Ratio

Fig. 8 Calculated stage performance characteristics to evaluate the effect of CCG

Table 3 Comparison between smooth casing stage and stages with circumferential casing grooves

	Stall mass flow	Efficiency at design point	Stall margin improvement
Smooth caing	41.5 g/s	73.50%	-
CCG_2mm	36.5 g/s	68.16%	12.05%
CCG_6mm	40.5 g/s	72.87%	2.41%
CCG_10mm	40.25 g/s	67.40%	3.01%

Flow fields at $\phi = 41.5\text{g/s}$, the stall point of the smooth casing stage

Circumferentially mass averaged static pressure plots and streamlines for the smooth casing stage and stages with CCG are shown in Figure 9. The adoption of CCG does not diminish the area of the large vortex at the impeller inlet. But as the fluid circulates in the grooves, the energy of the flow is dissipated. The area of the recirculation zone at the shroud side of the vaneless space reduces, and the center of the recirculation zone moves downstream. This will reduce the blockage in the tip region and hence improve the stall limit of the centrifugal compressor stage.

Figure 10 gives flow details and entropy distribution in the circumferential casing grooves. The stage with 10mm depth grooves shows the highest entropy value and consequently the lowest efficiency. As for the 2mm depth grooves, there is one single regular vortex in each of the grooves; the core of the vortex almost locates at the center of the groove. As for the 6mm depth grooves, the upper groove possesses two vortexes rotates at an opposite direction. The flow in the lower groove is irregular. In the upper groove of the 10mm depth grooves, two vortexes rotate at an opposite direction. The lower groove possesses one single vortex, but its core locates near the shroud side of the vaneless space. Thus a single regular vortex locating near the center of the grooves helps to improve the flow status in the stage, and contributes to the improvement of the stall limit of the stage.

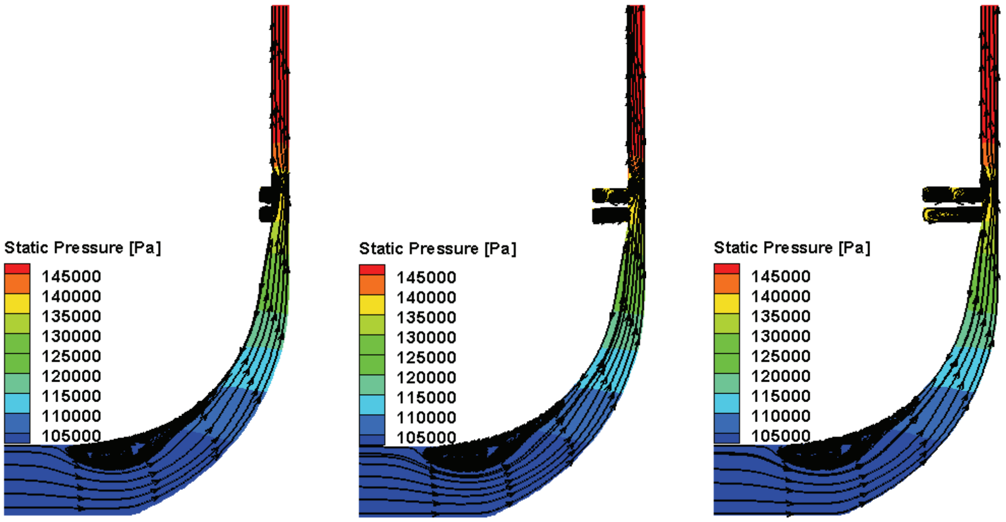

(a). CCG_2mm (b). CCG_6mm (c). CCG_10mm

Fig. 9 Streamlines and static pressure distribution at the meridional plane (Mass average)

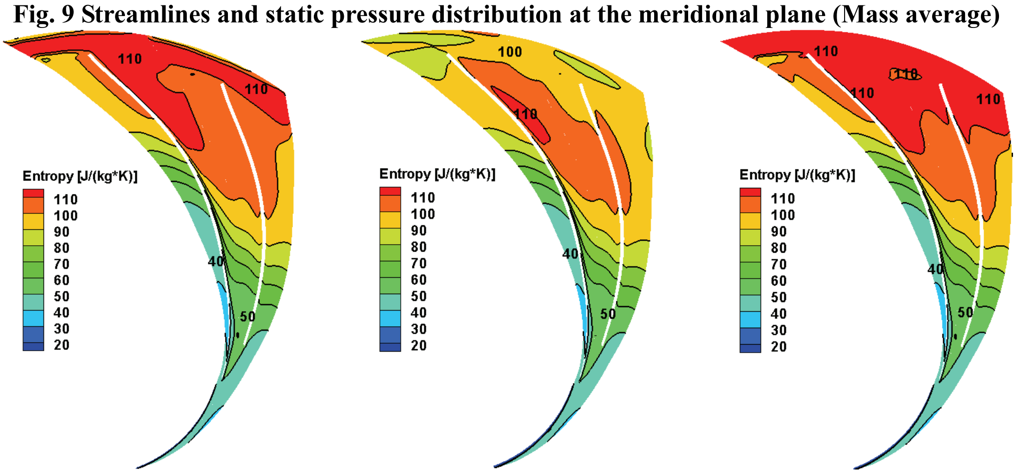

(a). CCG_2mm (b). CCG_6mm (c). CCG_10mm

Fig. 11 Entropy distribution in the impeller passage at 90% span

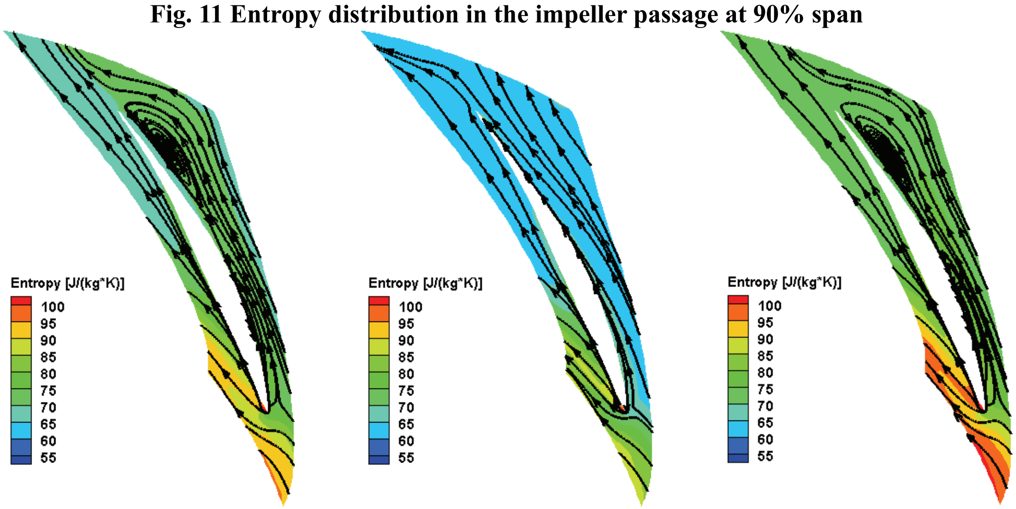

(a). CCG_2mm (b). CCG_6mm (c). CCG_10mm

Fig. 12 Streamlines and entropy distribution in the diffuser passage at 90% span

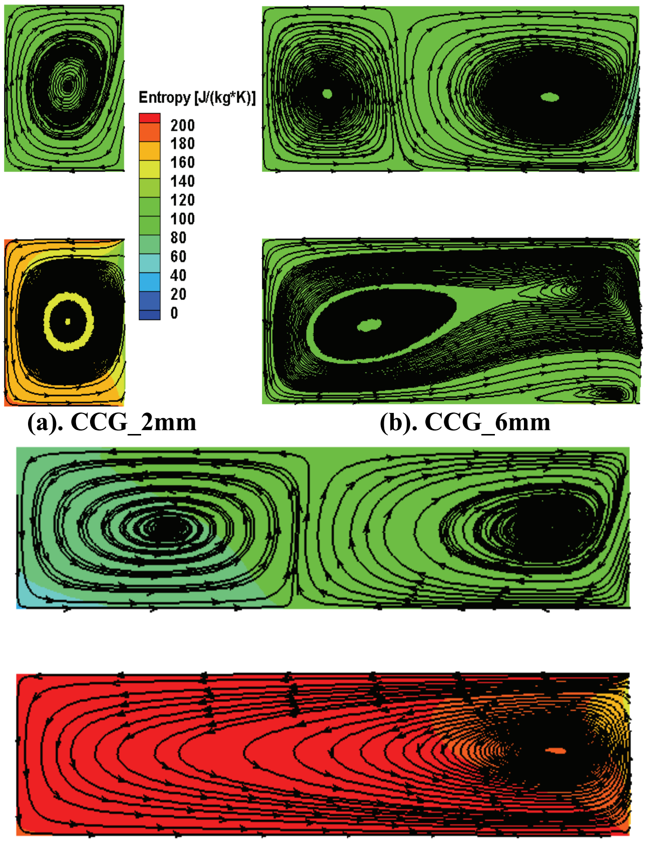

(a). CCG_2mm **(b). CCG_6mm**

(c). CCG_10mm

Fig. 10 Streamlines and entropy distribution in CCG (Mass averaged)

Figure 11 gives the entropy contours at 90% span in the impeller passage. The entropy distribution shows little change compared with the smooth casing stage in the fore part of the impeller passage. In the aft part and the outlet of the impeller passage, the situation changes. The loop flow and dissipation of the tip region fluid in the grooves cause the expansion of the high entropy zone for the stage with 2mm and 10mm depth grooves, indicating more losses in the impeller passage. For the stage with 6mm depth grooves, the high entropy region locating at the rear part of the pressure side of the main blade diminishes. But the entropy value in the impeller outlet increases.

The adoption of the 6mm depth grooves does not change the flow pattern at 90% span in the diffuser passage compared with the smooth casing stage as shown in Figure 12. But the entropy value increases throughout the diffuser passage, which indicates more losses. The adoption of the 2mm or 10mm depth grooves cause the flow to separate at the rear part of the diffuser vanes near the back arc side. The entropy value increases a lot throughout the diffuser passage.

CONCLUSIONS

Numerical investigations have been performed to study the role of different casing treatment devices in the enhancement of the operating range of a high speed centrifugal compressor stage. Several conclusions are drawn as follows:

Traditional inlet recirculation at impeller inlet does not enhance the stall margin of the compressor stage. As the adding of the extra device, the efficiency of the stage drops along the whole operating range. The efficiency of the stage with IR_2 drops more due to a longer flow path in the casing treatment device.

A new type vaneless space casing treatment with 2mm depth CCG expands the stall margin of the stage by 12.05%. However, its efficiency is lower than the stage with 6mm depth CCG, which only expand the stall margin by 2.41%. Its efficiency is also lower than the smooth casing stage.

Flow analyses indicate that the stall margin of the centrifugal compressor stages like the present one with a long and narrow diffuser passage is determined by the flow status in the diffuser passage. As the appearance of the 2mm depth grooves improves the flow status in the diffuser passage, the stall margin of the centrifugal compressor stage is extended dramatically.

Although the new type vaneless space casing treatment device is easy to implement, the preliminary result is not encouraging. The enhancement of the stall margin is accompanied with greater penalty of the performance of the stage.

For this reason, the CCG device has been redesigned, and the result is encouraging. An obvious enhancement of the stall margin has been obtained with minor efficiency penalty. Further analysis of the redesigned device is now undergoing, and the results will be discussed in the subsequent papers.

ACKNOWLEDGMENTS

This research is financially supported by the National Nature Science Foundation of China (Project No: 50725621 and No: 50976085).

REFERENCES

[1] Haupt, U., Abdel-Hamid, A. N., Kaemmer, N., and Rautenberg, M., 1986, "Excitation of Blade Vibration by Flow Instability in Centrifugal Compressors," ASME Paper No. 86-GT-283.

[2] Kwang-Jin Choi, Jin-Hyuk Kim, and Kwang-Yong Kim, 2010, "DESIGN OPTIMIZATION OF CIRCUMFERENTIAL CASING GROOVES FOR A TRANSONIC AXIAL COMPRESSOR TO ENHANCE STALL MARGIN," ASME Paper No. GT2010-22396.

[3] Hamid R. Hazby, Liping Xu, 2009, "ROLE OF TIP LEAKAGE IN STALL OF A TRANSONIC CENTRIFUGAL IMPELLER," ASME Paper No. GT2009-59372.

[4] Masahiro Ishida, Daisaku Sakaguchi, and Hironobu Ueki, 2006, "EFFECT OF PRE-WHIRL ON UNSTABLE FLOW SUPPRESSION IN A CENTRIFUAL IMPELLER WITH

RING GROOVE ARRANGEMENT," ASME Paper No. GT2006-90400.
[5] Koch, C. C., and Smith, L. H., 1968, "Experimental Evaluation of Outer Case Blowing or Bleeding of Single Stage Axial Flow Compressor. Part III-Performance of Blowing Insert Configuration No.1," NASA CR-54589, GE R68AEG318.
[6] Kenneth L. Suder, Michael D. Hathaway, Scott A. Thorp, et. al, "Compressor Stability Enhancement Using Discrete Tip Injection," Journal of Turbomachinery, 123(1), pp. 14-23.
[7] Michael D. Hathaway, "SELF-RECIRCULATING CASING TREATMENT CONCEPT FOR ENHANCED COMPRESSOR PERFORMANCE," ASME Paper No. GT2002-30368.
[8] Anthony J. Strazisar, Michelle M. Bright, Scott Thorp, et. al, "COMPRESSOR STALL CONTROL THROUGH ENDWALL RECIRCULATION," ASME Paper No. GT2004-54295.
[9] Aamir Shabbir, John J. Adamczyk, "Flow Mechanism for Stall Margin Improvement due to Circumferential Casing Grooves on Axial Compressors," Journal of Turbomachinery, 127(4), pp. 708-717.
[10] E. Brian Fite, "Fan Performance From Duct Rake Instrumentation on a 1.294 Pressure Ratio, 725 ft/sec Tip Speed Turbofan Simulator Using Vaned Passage Casing Treatment," NASA/TM-2006-214241.
[11] Jan Lepicovsky, Edward P. Braunscheidel, Gerard E. Welch, "Experimental Investigation of Rotating Stall in a Research Multistage Axial Compressor," NASA/TM-2007-214978.
[12] David Elliott, "The Potential Benefits of Advanced Casing Treatment for Noise Attenuation in Ultra-High Bypass Ratio Turbofan Engines," NASA/TM-2007-214812.
[13] Gary J. Skoch, "Experimental Investigation of Centrifugal Compressor Stabilization Techniques," NASA/TM-2003-212599.
[14] Gary J. Skoch, Mark A. Stevens, Thomas A. Jett, "DEVICES AND METHODS OF OPERATION THEREOF FOR PROVIDING STABLE FLOW FOR CENTRIFUGAL COMPRESSORS," US Pat. 7326027.
[15] Z. S. Spakovszky, "Backward Traveling Rotating Stall Waves in Centrifugal Compressors," Journal of Turbomachinery, 126(1), pp. 1-12.
[16] HU Liangjun, YANG Ce, QI Mingxu, et. al, "Numerical Investigation and Comparison on the Stall Improvement Mechanism of Centrifugal Compressor with Inducer Casing and Bleeding," Journal of Mechanical Engineering, 45(7), pp. 138-143 (In Chinese).
[17] M. T. Barton, M. L. Mansour, J. S. Liu, et al., "Numerical Optimization of a Vaned Shroud Design for Increased Operability Margin in Modern Centrifugal Compressors," Journal of Turbomachinery, 128(4), pp. 627-631.
[18] Junfei Yin, Penny Li, Stephane Pees, "OPTIMIZATION OF TURBOCHARGER PORTED SHROUD COMPRESSOR STAGES," ASME Paper No. GT2009-59248.
[19] Tong Wang, Wei Xu, Chuangang Gu, et al., "A NEW TYPE OF SELF-ADAPTIVE CASING TREATMENT FOR A CENTRIFUGAL COMPRESSOR," ASME Paper No. GT2010-23457.
[20] Subenuka Sivagnanasundaram, Stephen Spence, Juliana Early, et al., "AN INVESTIGAION OF COMPRESSOR MAP WIDTH ENHANCEMENT AND THE INDUCER FLOW FIELD USING VARIOUS CONFIGURATIONS OF SHROUD BLEED SLOT," ASME Paper No. GT2010-22154.
[21] Masahiro Ishida, Daisaku Sakaguchi, Hironobu Ueki, "OPTIMIZATION OF INLET RING GROOVE ARRANGEMENT FOR SUPPRESSION OF UNSTABLE FLOW IN A CENTRIFUGAL IMPELLER," ASME Paper No. GT2005-68675.
[22] Hideaki Tamaki, Masaru Unno, Tomoki Kawakubo, "AERODYNAMIC DESIGN TO INCREASE PRESSURE RATIO OF CENTRIFUGAL COMPRESSORS FOR TURBOCHAGERS," ASME Paper No. GT2009-59160.
[23] Hideaki Tamaki, "EFFECT OF RECIRCULATION DEVICE ON PERFORMANCE OF HIGH PRESSURE RATIO CENTRIFUGAL COMPRESSOR," ASME Paper No. GT2010-22570.
[24] Hiroshi Uchida, Akinobu Kashimoto, Yuji Iwakiri, "Development of Wide Flow Range Compressor with Variable Inlet Guide Vane," R&D Review of Toyota CRDL, 41(1), pp. 9-14.
[25] NUMECA International, 2007, "User Manual FINE/Turbo v8".
[26] NUMECA International, 2007, "User Manual AutoGrid v8".
[27] Takata H, Tsakada Y, "Stall margin improvement by casing treatment-its mechanisms and effectiveness," ASME Journal of Engineering for Power, 99(1), pp. 121-133.
[28] Xudong Huang, Haixin Chen, Song Fu, "CFD Investigation on the Circumferential Grooves Casing Treatment of Transonic Compressor" ASME Paper No. GT2008-51107.
[29] Niazi S., Stein A., and Sankar L. N., "Computational Analysis of Stall Control Using Bleed Valve in a High-Speed Compressor," AIAA Paper 2000-3507.